Trends in heat and cold wave risks for the Italian Trentino Alto-Adige region from 1980 to 2018

Martin Morlot[1], Simone Russo[2], Luc Feyen[2], and Giuseppe Formetta[1]

[1] University of Trento, Department of civil, environmental, and mechanical engineering,

5   via Mesiano, 77, 38123, Trento (Italy)

[2] European Commission, Joint Research Centre

Corresponding author: Giuseppe Formetta, giuseppe.formetta@unitn.it

Abstract

Heat waves (HWs) and cold waves (CWs) can have considerable impact on people.

10   Mapping risks of extreme temperature at local scale accounting for the interactions between hazard, exposure and vulnerability remains a challenging task. In this study, we quantify risks from HWs and CWs for the Trentino-Alto Adige region of Italy from 1980 to 2018 at high spatial resolution. We use the Heat Wave Magnitude Index daily (HWMId) and the Cold Wave Magnitude Index daily (CWMId) as the hazard indicator.

15   To obtain HWs and CWs risk maps we combined: i) occurrence probability maps of the hazard, ii) normalized population density maps, and iii) normalized vulnerability maps based on eight socioeconomic indicators. The occurrence probability of the hazard is obtained using the Tweedie zero-inflated distribution. The methodology allowed us to disentangle the effects of each component of the risk to its total change.

20   We find a statistically significant increase in HWs hazard and exposure while CWs hazard remained stagnant in the analyzed area over the study period. A decrease in vulnerability to extreme temperature spells is observed trough the region except in the

larger cities where vulnerability has increased. HWs risk increased in 40% of the region, with it being stronger in highly populated areas. Stagnant CWs hazard and declining

25 vulnerability result in reduced CWs risk levels, with exception of the main cities where it grew due to their increased vulnerabilities and exposures.

The findings of our study are relevant to steer investments in local risk mitigation, and this method can potentially be applied to other regions that have similar detailed data.

1   Introduction

30 Heat waves (HWs) and cold waves (CWs) are hazards that affect public health and the environment (Gasparrini et al., 2015; Habeeb et al., 2015). With global warming, HWs intensities and durations are expected to increase while those of CWs are expected to decrease (Perkins-Kirkpatrick and Gibson, 2017; Russo et al., 2015; Smid et al., 2019), which would change their risks to society. A recent report showed that in the year 2018

35 worldwide, 157 million more people were exposed to HWs compared to the year 2000 (Watts et al., 2018). In Europe, recent high intensity HWs events (2003 and 2018, where HWs are defined as 3 days over 90th temperature percentile of the 1980-2010) have impacted as much as 55% of its area (García-León et al., 2021). In Italy, HWs have had a strong impact on mortality such as in 2003 when a 27% mortality increase

40 was reported over August, while in 2015 there was a 23% increase in July, compared to the 5 previous years (Michelozzi et al., 2005, 2016). In Trentino Alto-Adige (our study region), Conti et al. (2005) showed that for the large HW of 2003, mortality increased by 32% in Trento and 28% in Bolzano (the region's two main cities) compared to the previous year. In the city of Bolzano, it was also found that higher hospital admissions

45 occurred during HWs events particularly among elderly women (Papathoma-Köhle et

al., 2014). With regards to CWs in Europe, recent winters have claimed 790 deaths in 2006 and 549 deaths in 2012 (Kron et al., 2019). The increase in mortality and among elder people is also found in Italy for CWs. For example, de'Donato et al., (2013) reported a notable increase in mortality (47%) for the timeframe of the 2012 CW in the

50 city of Bolzano.

HWs and CWs events clearly come with a risk but how do we define this risk? The United Nations Office for Disaster Risk Reduction (UNDRR, 2021) and the Intergovernmental Panel on Climate change (IPCC, 2014) define risk as a function of hazard, exposure, and vulnerability. Exposure is defined as people, infrastructure,

55 housing, production, and other tangible human assets present in hazard-prone areas. Vulnerability is defined as the conditions that define the susceptibility of an individual, infrastructure, or a community to be impacted by the hazard. To successfully quantify risk, one must be able to measure all three components: hazard, exposure, and vulnerability.

60 With regards to hazard and exposure, several temperature hazard-exposure studies have been conducted at global (e.g. Chambers, 2020; Dosio et al., 2018), continental (eg. King et al., 2018), or city-scale (e.g. Smid et al., 2019). Most studies focus on human exposure (eg. Chambers, 2020; Tuholske et al., 2021) and on the exposure of land areas (e.g., Ceccherini et al., 2017; Oldenborgh et al., 2019; Russo et al., 2016).

65 These studies found increasing trends in HWs (Chambers, 2020; Dosio et al., 2018) and decreasing trends in CWs in their period of analysis (Oldenborgh et al., 2019, Smid et al., 2019).

Most studies on HWs and CWs have used qualitative numerical thresholds on the indicator to define severity and exposure to the hazards. However, extreme events are usually defined by their return periods. In the case of HWs and CWs fitting extreme value distributions to define the return periods is difficult due to the possible absence of events in the analyzed time frame (i.e. zero values, in the case where there are no HWs/CWs in a given year). Generalized extreme value distribution (GEV) and non-stationary-techniques (Dosio et al., 2018; Kishore et al., 2022; Russo et al., 2019) have enabled to estimate HWs and CWs' return periods, but both approaches did not explicitly account for the zero presence in the analyzed time series.

Instead, for the first time we use the zero-inflated distribution of Tweedie families (Jorgensen, 1987; Tweedie, 1984) to estimate HWs and CWs frequency of occurrence, which enabled us to directly account for the possible zero values. The Tweedie distribution has been used mostly for the purpose of insurance claims analysis, but has seldom been applied in the field of natural hazards, such as HWs mortality (Kim et al., 2017), droughts (Tijdeman et al., 2020), and rainfall analysis (Dunn, 2004; Hasan and Dunn, 2011). The main advantage of the Tweedie distribution is the possibility of considering many distributions for the continuous and semi-continuous domain such as: normal, Gamma, Poisson, Compound Gamma-Poisson, and Inverse Gaussian (Bonat and Kokonendji, 2017; Rahma and Kokonendji, 2021; Shono, 2008; Temple, 2018). Moreover, for some of these distributions (i.e. Poisson mixtures of gamma distributions) it explicitly enables the fitting of zero-inflated data. Tweedie distribution main limitation is the complex distribution's fitting methodology and the difficulties to compare it to other models via information criteria such as the Akaike's information criterion (Shono, 2008).

To perform a risk analysis, the vulnerability to the hazard must be quantified. HWs and CWs vulnerabilities can be approximated by combinations of several socioeconomic indicators. At the community level in the United States, factors such as social isolation, presence of air conditioning, proportion of elderly and proportion of diabetics in the

95 population were found to be key for human vulnerability to temperature extremes (Reid et al., 2009). In Korea at the county level, Kim et al. (2017) found that elderly living alone, agricultural workers and unemployed are the main indicators for vulnerability to heat wave days and tropical nights. Temperature vulnerability has also been appraised at city scale for HWs mortality (Ellena et al., 2020) and at regional scale (López-Bueno

100 et al., 2021) for CWs mortality. Karanja & Kiage (2021) and Cheng et al. (2021) provide an overview of the different types of indicators used in the literature to quantify vulnerability. The indicators can be diverse, ranging from population structure (e.g., age and health characteristics), social status, economic conditions, community (cultural) group characteristics, and household physical characteristics. Studies on social

105 vulnerability to natural hazards in Italy used a diversity of indicators derived from the census records (Frigerio and De Amicis, 2016).

HWs and CWs risks are often assessed using different methodologies depending on the objectives of the study. On a global scale, Russo et al., (2019) establish a risk index using the probabilities of HWs as hazard, where the exposure is the population density

110 normalized in [0;1] based on its maximum, minimum values; while vulnerability is based on a socio-economic indicator (human development index). For Italy, Morabito et al (2015) conducted a risk analysis of heat on elderly in the major cities, using the elderly

population as the only vulnerability factor and summer average temperatures for the period 2000-2013 to quantify the hazards.

115 Assess the risk associated to extreme temperatures in the Italian Trentino Alto-Adige region is a relevant social and scientific objective given: i) the increase in the percentage of elderly people (i.e. vulnerability change) (Papathoma-Köhle et al., 2014) and ii) the changing temperature extremes in view of climate change (i.e. changing hazard).

120 Few studies have attempted to quantify HWs and CWs impacts for the Trento and Bolzano cities (main cities of the region), such as Conti et al. (2005) as part of their studies on Italian cities and Papathoma-Köhle et al. (2014) who studied impacts in Bolzano. The former compared the mortality data of the year 2003 (affected by the very intense HW) to the year 2002, finding an increase of morality in both Trento and

125 Bolzano. The latter compared the hospital admissions due to HWs in summer months of three years (2003, 2006, and 2009) possible heat health issues among elder women.

To better understand the spatiotemporal evolution of HWs and CWs human risk and to plan adequate risk-mitigation measures in the region, there is a need to assess the risk and its change at high spatial and temporal resolution.

130 The aim of this article is to solve some of these previous limitations while quantifying HW and CW hazards, the human exposures, vulnerabilities, and risks at the high-definition (i.e. city-scale) over the period 1980-2018, for the Trentino-Alto-Adige region. The goals for this paper are therefore as follow:

1) Quantify HWs and CWs hazards and their return level at a very high spatial resolution (250m) by combining for the first time i) the indicators proposed by Russo et al., (2015) and Smid et al., (2019), together with ii) the Tweedie distribution;

2) Quantify human exposures and vulnerabilities to HWs and CWs and their evolution in time for the Trentino-Alto-Adige region;

3) Quantify the HWs and CWs risks across the region and understand their main drivers by disentangling the contribution of the risks' components to its change.

2 Study Area

*The Trentino Alto-Adige region (*Figure 1: The Trentino Alto-Adige region and its most populated cities (Trento, Bolzano, Rovereto and Merano); the colors indicating the elevations, river network, and lakes.

) is a mountainous region in northern Italy, which borders Austria. The elevation of the region varies from 65m for lake Garda to 3,439m for Lagaunspitze. It is composed of two provinces (Province of Trento and Province of Bolzano). Its most populous cities (population for 2022 in parenthesis) are the two provincial capitals, Trento (118509) and Bolzano (107025), as well as minor cities such as Merano (40994) and Rovereto (39819). The main rivers in the region are the Adige, and its tributary, the Isarco. Due to its diverse geography, the climate is also diverse ranging from Subcontinental to Alpine on the Koppen classification (Fratianni and Acquaotta, 2017).
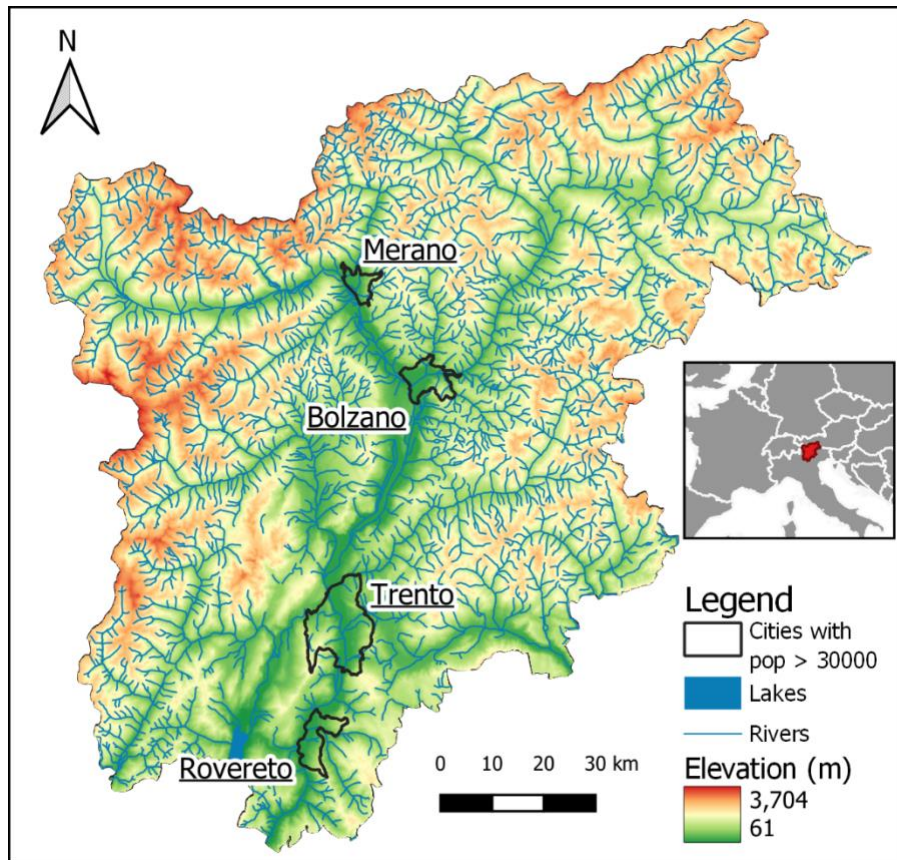
Figure 1: The Trentino Alto-Adige region and its most populated cities (Trento, Bolzano,

155   Rovereto and Merano); the colors indicating the elevations, river network, and lakes.

3   Methodology

3.1   Temperature data

In order to quantify the HWs and CW hazard, we used the freely available spatial

temporal temperature dataset by Crespi et al. (2021). It consists of gridded daily

160   temperatures for the entire Trentino Alto-Adige region covering the period of 1980-2018

at a resolution of 250 meters. This dataset is based on more than 200 station daily

records which have been quality controlled and homogenized. The interpolation method

is based on a combination of 30-year temperature climatology (1981–2010), daily

anomalies and explicitly accounts for topographic features (i.e. elevation, slope) which

165   are crucial in orographic complex areas such as the Trentino Alto-Adige. The leave one

out cross validation presented in Crespi et al. (2021) finds mean correlation coefficient

higher than 0.8 and mean absolute errors of around 1.5 degree Celsius (on average

across months and stations used for the interpolation).

The hazard analysis presented in this paper rely on the Crespi et al. (2021) air

170   temperature database. Although it is based on a state-of-the-art interpolation approach

and it represents the best product for the area, more attention should be given to

measuring meteorological variables in orographically complex area and at high

elevation. This will in turn reduce the uncertainty in spatial interpolation and improve the

quantification of impacting hazards such as HWs and CWs.

175   **3.2   Hazard quantification and distribution fitting**

3.2.1 Hazard quantification

To quantify the hazard we used the HWMId (Russo et al., 2015) and the CWMId (Smid

et al., 2019). These indices represent a way of measuring extreme temperature events

while considering their durations, intensity, and taking in account the site-specific

180   historical climatology (30years).

According to Russo et al. (2015), HWMId is defined as the maximum magnitude of the

HWs in a year. A HW occurs when the air temperature is above a daily threshold for

more than three consecutive days. The threshold is set to the 90th percentile of the

temperature data of the day and the window of 15 days before and after throughout the

185   reference period 1981-2010. The magnitude of a HW is the sum of the daily heat

magnitude $\mathrm{HM_d}$ of all the consecutive days composing the HW (Equation 1):

$$HM_d(T_d) = \begin{cases} \dfrac{T_d - T_{30y25p}}{T_{30y75p} - T_{30y25p}} & \text{if } T_d > T_{30y25p} \\ 0 & \text{if } T_d \le T_{30y25p} \end{cases}$$

(1)

where $HM_d(T_d)$ corresponds to the daily heat magnitude, T_d the temperature of the day in question and T_{30y25p} and T_{30y75p} correspond to the 25th and 75th percentile of the yearly maximum temperature for the 30 years of the reference period (1981-2010). The interquartile range (IQR, i.e. the difference between the T_{30y75p} and T_{30y25p} percentiles of the daily temperature) is used as the heatwave magnitude unit and represents a non-parametric measure of the variability of the temperature timeseries. Therefore, a value of HM_d equals to 3 means that the temperature anomaly on day d with respect to T_{30y25p} is 3 times the IQR. Finally, for a given year HWMId corresponds to the highest sum of magnitude (HMd) over the consecutive days composing a heatwave event (with only days with HMd > 0 considered).

Analogously to the HWMId, CWMId is defined as the minimum magnitude of the CWs in a year (Smid et al., 2019). A CW occurs when the air temperature is below a daily threshold for more than three consecutive days. The threshold is set to the 10th percentile of the temperature data of the day and the window of 15 days before and after throughout the reference period 1981-2010.

The daily cold magnitude corresponds to (Equation 2):

$$CM_d(T_d) = \begin{cases} \dfrac{T_d - T_{30y75p}}{T_{30y75p} - T_{30y25p}} & \text{if } T_d < T_{30y75p} \\ 0 & \text{if } T_d > T_{30y75p} \end{cases}$$

where $CM_d(T_d)$ corresponds to the cold daily magnitude, T_d the daily temperature and T_{30y25p} and T_{30y75p} correspond to the 25th and 75th percentile yearly temperature for the 30 years used as a reference. Inversely to HWMId, the lowest cumulative magnitude sum is retained for each year and with only consecutive days with $CM_d < 0$ considered to calculate it. CWMId being always <T 0, its absolute values are retained for its values to be on a positive interval (similar to HWMId).

3.2.2 Distribution fitting

The HWMId and CWMId yearly values are fitted with a probability distribution to estimate their return periods. Considering that HWMId and CWMId are both defined in [0,+Inf[, we use the Tweedie distribution (Jorgensen, 1987; Tweedie, 1984), a distribution that can act as zero-inflated, thus accounting for the presence of zeros directly. The Tweedie distribution is an exponential dispersion model which has a probability density function of the form (equation 3):

$$f(y, \theta, \Phi) = a(y, \Phi) * \exp\left[\frac{1}{\Phi}\{y\theta - \kappa(\theta)\}\right]$$

(3)

where Φ corresponds to its dispersion parameter that is positive, θ to its canonical parameter, and $\kappa(\theta)$ the cumulant function. The function a(y, Φ) generally cannot be written in closed form. The cumulant function is related to the mean ($\mu_y = \kappa'(\theta)$) and variance ($\sigma_y = \Phi * \kappa''(\theta)$) and in the case of a Tweedie distribution the variance has a power relationship with the mean (Equation 4):

$$\sigma_y = \Phi * (\mu_y)^p$$

(4)

where p corresponds to the power parameter that is positive.

230 Depending on the value of p, the distribution will behave differently. In the case where p
is between 1 and 2, it belongs to the compound Poisson-gamma distribution with a
mass at zero, while other p values can make the distribution correspond to a normal,
Poisson, or gamma distribution, among others. The use of the Tweedie distribution is
retained as it permits to consider the zero values, while also considering other

235 distributions should there be an absence of zero values.

We fit the distribution to the previously found HWMId and CWMId values with the help
of the Tweedie R package (Dunn, 2021). It provides distribution density, distribution
function, quantile function, random generation for the Tweedie distributions. The
Tweedie parameters (i.e. mean, power, and dispersion) have been estimated by the

240 "tweedie.profile" function (Dunn, 2015) using the maximum likelihood as described by
Dunn (2015) and Dunn and Smyth (2005). An example of the fitted distribution for
Bolzano and Trento can be found in the supplementary material (Figure S1). It is also
possible to use the same package to estimate a quantile using the fitted distribution.
This enables to estimate specific return levels for return periods T for both HWMId and

245 CWMId. For this study two return levels are retained, 5 years (HW5Y for HW, and
CW5Y for CW) and 10 years (HW10Y for HWs and CW10Y for CW). This choice aims
to account for of both the length of the analyzed period (39 years) and the type of
hazards we are analyzing (HWs and CWs usually doesn't occur every year). Higher

return level estimations would be affected by extrapolation effects and higher

250 uncertainty.

For statistical fit verification, the Kolmogorov–Smirnov (KS) test on two samples is used with one sample being the found HWMId or CWMId values, and the other sample being a randomly generated sample using the fitted distribution value. This goodness of fit of test is one of the most commonly used in the literature for the case of the corresponding

255 zero inflated Tweedie distribution (Goffard et al., 2019; Johnson et al., 2015; Rahma and Kokonendji, 2021). The null hypothesis of this test is that the two sample belong to the same distribution. If the P-value for this test is below the significance level α of 5%, the null hypothesis is rejected, otherwise we cannot reject the null hypothesis at this significance level.

260 **3.3   Exposure quantification**

To quantify the population exposed to HWs and CWs, we use time-varying population data from the Global Human Settlement Layer (GHSL) (Schiavina et al., 2019). The population data is available at a resolution of 250m for the following years: 1975, 1990, 2000 and 2015. Both this data, and the population count done by the Italian national

265 statistical institute, indicate a growing population throughout the region (overall 23%).

To more accurately model exposure, we created yearly varying population maps for the period 1980-2018 following the methodology presented in other studies (e.g. Formetta and Feyen, 2019; (Neumayer and Barthel, 2011). We linearly interpolated the data in time for the period 1980 to 2015 (assuming a constant rate in between available years)

270 and we used the closest year for the period 2016-2018.

Following recent studies (King & Harrington, 2018; Russo et al., 2019), for each year, a pixel is considered exposed to HW/CWs hazard (or to a 5 or 10 year return-period HWs/CWs) if for that year the HWMId/CWMId of the pixel is greater than zero (or greater than the corresponding return level HW5Y/CW5Y or HW10Y/CW10Y, respectively).This is the exposition factor, and it is a binary value (0 meaning not exposed or 1 meaning exposed).

The percentage of population exposed are calculated on annual basis over the study period (1980-2018) with the help of population data linearly interpolated from 1980 to 2018.

Using this population data, percentage of population exposed are then calculated using the following equation (Equations 5 and 6):

$$Population\ exposed(t) = \sum_i EF_i * population_i(t)$$

(5)

$$Percentage\ of\ population\ exposed\ (t) = \frac{Population\ exposed(t)}{Total\ population\ (t)}$$

(6)

where i corresponds to the pixels, t to the year being analyzed, EF to the exposition factor mentioned above (binary).

3.4 Vulnerability quantification

We express HWs and CWs vulnerability using eight indicators as in Ho et al. (2018), who quantify community vulnerability to HWs and CWs events based on extreme age,

household physical characteristics, social status and economic conditions. The list of variables considered are reported in Table 1.

Table 1: Vulnerability indicators used (after Ho et al., 2018)

Category	Indicator	Definition
Extreme Age	Older Age	Population over 55 years old
	Infants	Population under 5 years old
Household physical characteristics	People in old houses	Percentage of household living in housing built prior to 1960 (corresponding to when better insulation started being implemented)
	People in poor living condition	Percentage of household living in other type of housing not meant for inhabitation (cellar, attics)
Social Status	Low education population	Population with low education (no middle-school diploma)
	People living alone	Number of single-person households

	Low-income population	Population in a household with children and no money-earning members
Economic Status		
	Unemployed	Unemployment rate

295 The spatially varied indicators are freely available in the census records (i.e. sub-city

level) from the Italian national statistical institute (ISTAT, 2021) for three different years

(1991, 2001 2011). Given the data time constraints, vulnerability is thus derived for

those years only.

The methodology to quantify vulnerability uses the equal weight analysis (EWA, e.g. Liu

300 et al, 2020). Firstly, the individual indicators are standardized between 0 and 1, prior to

aggregation (their sum); the standardization is done at the city level for all the years of

record (1991, 2001, 2011) based on Equation 7:

$$\text{Standardized Indicator } (t) = \frac{\text{Indicator}(t) - \min(\text{Indicator}_{1991,2001,2011})}{\max(\text{Indicator}_{1991,2001,2011}) - \min(\text{Indicator}_{1991,2001,2011})}$$

305 (7)

Secondly, the EWA is performed according to Equation 8:

$$\text{Vulnerability } (t) = \frac{\sum \text{Standardized indicator}(t)}{\text{number of indicators}}$$

(8)

310 This approach was chosen as it is the simplest method for weighing the vulnerability indicators and it is commonly applied in the literature with regards to HWs and CWs (e.g. Buscail et al., 2012; Buzási, 2022).

Finally, we created yearly varying vulnerability maps for the period 1980-2018 following the same approach we used for the population.

315 **3.5 Risk Quantification**

Risk here is assumed to be a function of hazard, exposure and vulnerability, which are multiplied to quantify risk (UNDRR, 2021). This is one of the two most commonly used approaches in literature (Dong et al., 2020; Quader et al., 2017; Russo et al., 2019), with the other approach being the addition of the different risk components.

320 Multiplication when compared to addition is found to better highlight the complex relationship between the different components, as the multiplication of the multivariate probabilities of independent variables follow a product law (El-Zein and Tonmoy, 2015; Estoque et al., 2020; Peng et al., 2017).

The risk is calculated as per Dong et al. (2020) (equation 9):

325
$$\text{Risk} = \sqrt[3]{\text{Hazard} * \text{Exposure} * \text{Vulnerability}}$$

(9)

with each of the risk components having a value in [0,1]. The hazard is computed as the probability of occurrence of HWs/CWs by using the fitted Tweedie distributions probability function for each pixel. Exposure is the standardized population density. The

330 vulnerability derived from standardized variables is also between [0,1]. The resulting risk

is therefore also bound by 0 and 1, with 0 corresponding to the lowest level of risk and 1 to the highest level of risk.

The risk is calculated at the municipality level because it is the lowest level of resolution of the three elements that compose it.

335 In order to further investigate which are the driving factors of the risk, we disentangle the marginal effect of each component (i.e. hazard, exposure, and vulnerability) for both HWs and CWs. In turn, one of them is allowed to vary across 1980-2018 and two of them are kept constant (to their value at the year 2003, the middle of the analyzed period).

340 **3.6 Trends analysis & statistical significance**

The trends are analyzed using the robust regression technique (Huber, 2011). This method is often used throughout the literature for natural hazards (Formetta and Feyen, 2019; Kishore et al., 2022).

The trends are analyzed using the robust regression technique (Huber, 2011). This

345 method is often used throughout the literature for assessing trends in natural hazards (Formetta and Feyen, 2019 for multiple hazards and Kishore et al., 2022 specifically for HWs). To confirm the statistical significance of the trends the false discovery rate (FDR) methodology is used according to Wilks (2016) and Leung et al. (2019), with a significance level $\alpha=0.05$. The FDR is defined as the statistically expected fraction of

350 null hypothesis test rejections at the grid cell for which the respective null hypotheses are actually true (Wilks 2016).

4   Results

4.1   Hazard quantification and trends

For HWs hazard intensities, the most notable year on record (1980-2018) in the region

is 2003, where HWMId reached a pixel maximum of 30.4 and a median value of 16.9

over the area (Figure S2 in the supplementary material). The second most intense HW

occurred in 2015 and the third most intense in 1983. From the six years with the highest

median HWMId between 1980 and 2018, four occurred in the last decade (2010, 2013,

2015, 2017), suggesting that climate change is already increasing the frequency of heat

waves in the Trentino Alto-Adige region. For CW, only 1985 stands out, with a

maximum and median CWMId of 27 and 14.5, respectively, or nearly three times more

than that of any other year on record. The second strongest cold wave occurred in

2012.

A KS test (Figure S3 in the supplementary material) shows that the Tweedie distribution

provides a good fit for both CWMId and HWMId, with power parameter values between

[1,2] for the entire region. The KS goodness of fit test reveals a significance level of

α_{sig}=5% as well as the false discovery rate for the significance level $2\alpha_{sig}$ for any pixel in

the region. This permits us to estimate return levels for both HWs and CWs and analyze

trends based on them. The return levels for return periods of 5 years (HW5Y, CW5Y)

and years (HW10Y, CW10Y) for every pixel are shown in Figure S4 in the

supplementary material.

Fitting the robust linear model to the HWs values, statistically significant positive trends

are found for HWs (i.e. HWMId > 0) and HWs with a magnitude larger than the 5-year

event (HWMId > HW5Y) in most pixels of the region (Figure 2**Error! Reference source**

375 **not found.**). For rarer events, those larger than the 10-year event (HWMId > HW10Y),

no statistically significant increase in HWs intensity are found in the region. With

regards to the location of these trends, some of the highest parts of the regions have

the greatest coefficient of increase (north of Bolzano and in the mountains located

north-west of the region). For all CWs, we do not find statistically significant trends in

380 any part of the region.

Figure 2: Trends in heat waves (HWs) and cold waves (CWs) using the robust linear

model based on yearly HWMId and CWMId magnitudes from 1980 to 2018 for HWs a)

with HWMId > 0, b) with HWMId > HW5Y, c) HWMId > HW10Y and for CWs and d) with

385 *CWMId > 0, e) with CWMId > CW5Y, f) CWMId > HW10Y*
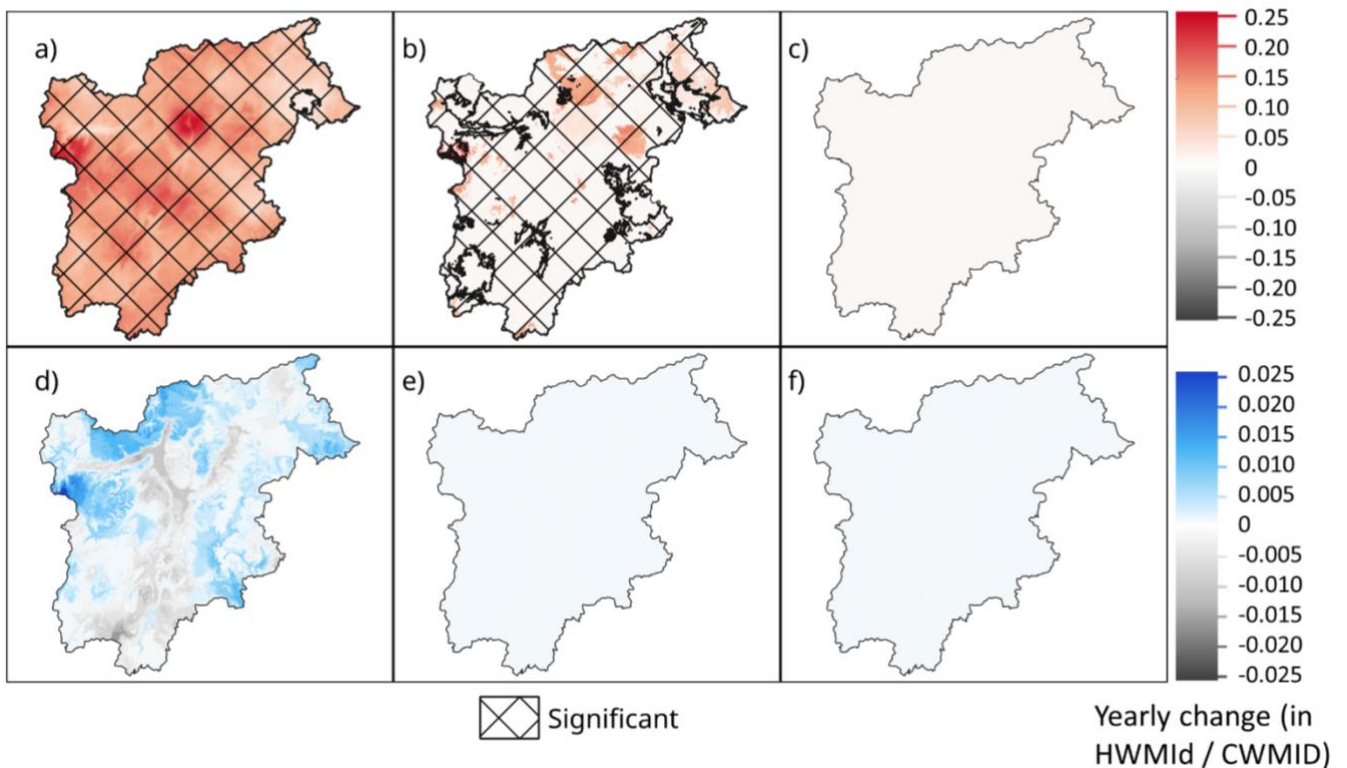
4.2 Population exposure

In total, between 1980 and 2000, in the study region, about 900 000 people were exposed to a 5-year HW event, 250 000 to 10-year HW event, 3million to 5-year CW event and 1.9 million to 10-year CW event. Between 2000 and 2018, the values

390 increased to over 5millions for 5-year HW event and to about 2.5million for 10-year HW event but decreased to 2.4 million for 5-year CW event and to 500 000 for 10-year CW event. However, due to the importance of the demographic change in the region (increase of population by 23%), it is important to study the percent of population impacted by these different events to understand whether these changes are due to

395 demographic changes or the change in the frequency of events.

Figure 3**Error! Reference source not found.** presents the share of the population exposed to HWs and CWs intensities larger than those of 5-year and 10-year events over the period 1980 to 2018 on a yearly basis. It shows that a higher share of the population was exposed to HWs more frequently after 2000 compared to the first two

400 decades (80s and 90s). For both return periods, the robust linear model indicates a significant increase in population exposed to HWs over the region with a coefficient for the increase of nearly 1% per year for HWs>HW5Y and 0.02% for HWs>HW10Y. We did not find a significant trend in human exposure to CWs in the region.
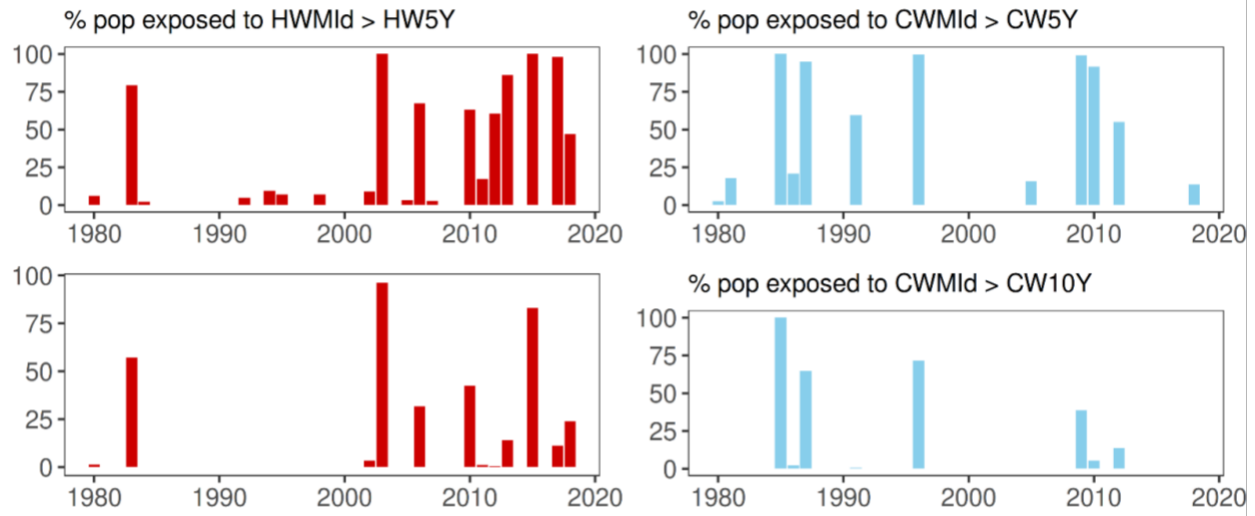
405

Figure 3: Percentage of population exposed to heat wave and cold wave events greater than the return levels of 5years and 10years over the span of 1980-2018

4.3 Vulnerability quantification

410 The vulnerability for the region (Figure 4: Calculated extreme temperatures vulnerability index for the three years of the census records (1991, 2001, 2011) with the borders of the municipalities in black) decreases in time, with an average value of 0.42 in 1991, 0.32 in 2001 and 0.27 in 2011. The main reason for the decrease in vulnerability at regional scale is the improvement in overall education level and housing conditions (i.e., fewer people living in old and poor housing conditions). However, by contrast, for the

415 larger cities (those with a population over 30,000: Merano, Bolzano, Trento, Rovereto), the vulnerability has increased from 0.28 in 1991 to 0.30 in 2001 and 0.32 in 2011, averaged for those cities (see Figure S5 In the supplemental material). The increase in these cities' vulnerability relates to the older age indicator and social status, with a growing portion of the population above 55 and an increase in the number of isolated

420 households (i.e., people living alone).
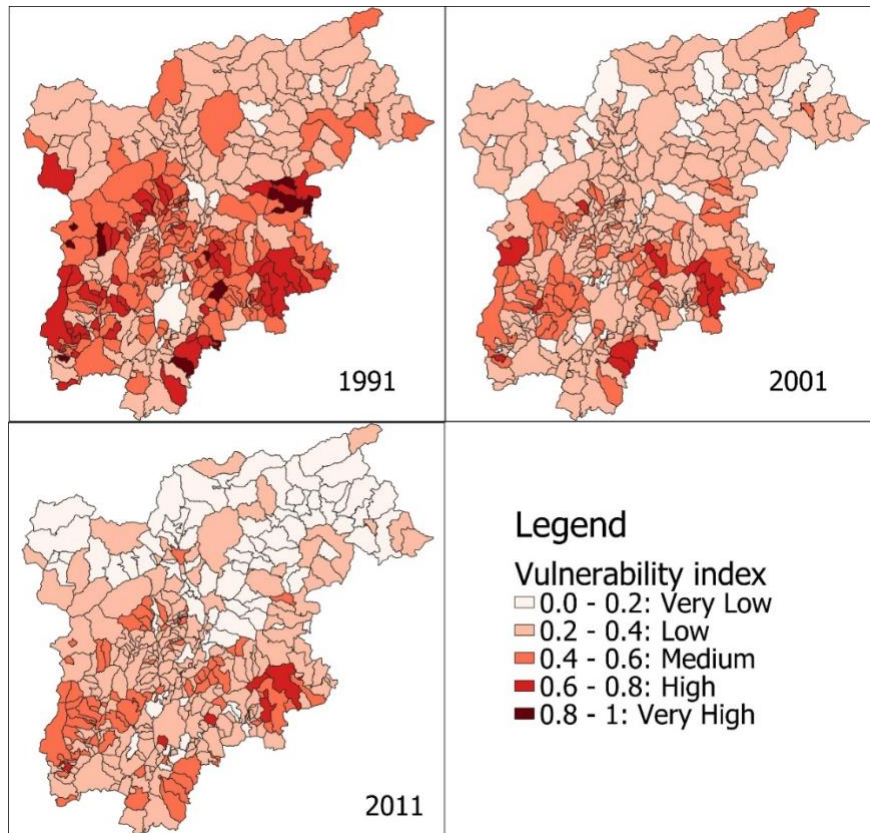
Figure 4: Calculated extreme temperatures vulnerability index for the three years of the census records (1991, 2001, 2011) with the borders of the municipalities in black

425 **4.4   Risk quantification**

Error! Reference source not found. Figure 5 shows the trend in risk for the whole region over the period 1980-2018. The robust linear model shows significant increasing trend in HWs risk in 40% of the area, with a significant decreasing risk in some isolated parts of the region of study. While the risk from CWs has decreased over most of the

430   region since the 1980s, in the major cities (Trento, Rovereto, Bolzano and Merano) we found an increase in CWs risk.

Decadal means of the annual regional risk values confirm these trends, with the HWs risk increasing from 0.119 in the 1980s to 0.133 for the 2010s, while CWs risk has decreased from 0.134 in the 1980s to 0.124 in the 2010s. Decadal means of HWs risk

435   for the large cities show a stronger trend compared to the whole region. We found that the average HWs risk in the main cities increased by nearly 45% compared to the 12%
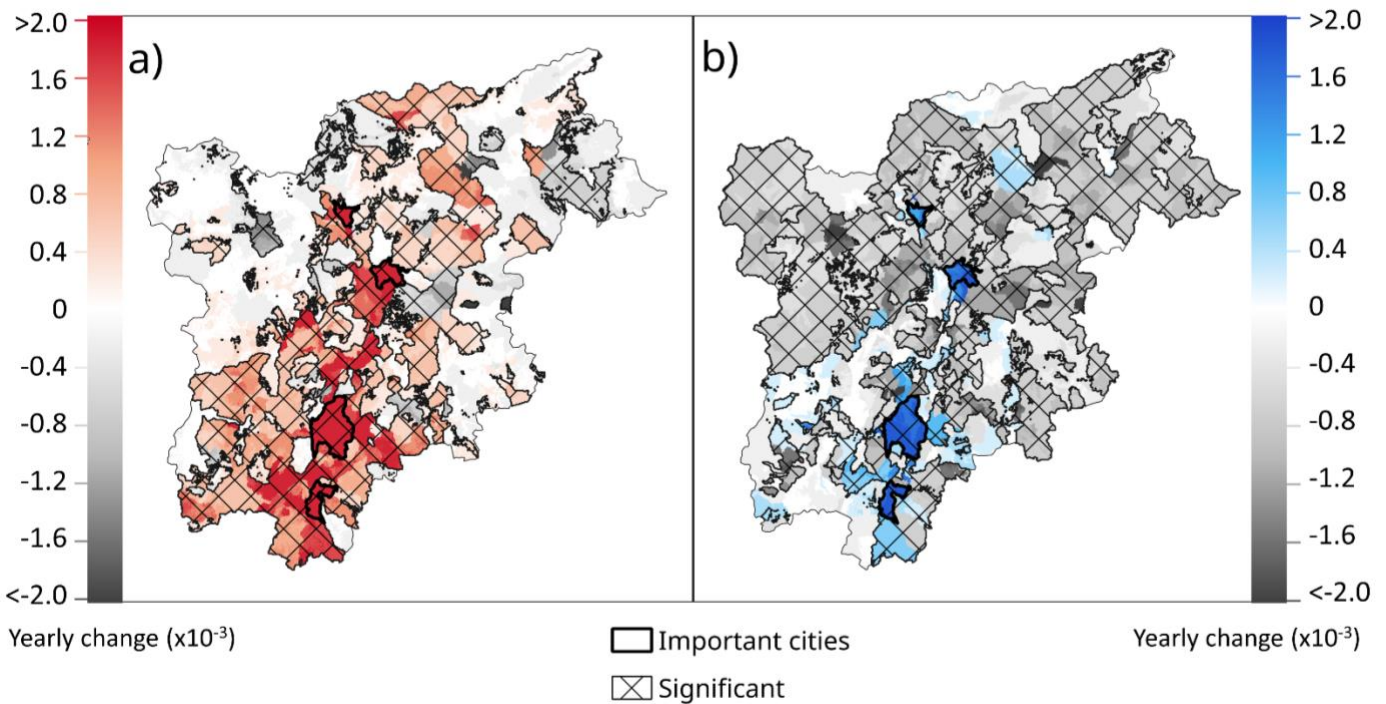
increase in the whole region. Decadal means of CWs risk for the main cities increased by nearly 17% whereas in the whole region, it decreased by 7%.

Figure 5: Trends of a) heat waves and b) cold waves risks using the robust linear

440   *method, colors indicating an increase in the risk and grey a decrease, significance is indicated with the hashing, the yearly change being the robust linear model coefficient.*

The highest annual risk levels for both HWs and CWs coincide with the years with the highest hazard intensity (2003 for HW and 1985 for CW, see Figure S6 in the

supplementary material), indicating that the hazard is potentially the main factor for risk.

445   However, risks are further modulated by exposure and vulnerability. The risks are found

to be the highest in the largest cities (Bolzano, Merano, Rovereto and Trento).

Figure 6 shows the marginal effect of the driving factor behind the trends in HWs and

CWs risks. Figure 6-a, Figure 6-c, and Figure 6-e (Figure 6-b, Figure 6-d, and Figure 6-

f) show the trend in HWs (CWs) risks with only vulnerability, only exposure, and only

450   hazard changing, respectively.

The results in Figure 6-a and Figure 6-b show the same patterns as well as Figure 6-c

and Figure 6-d because exposure and vulnerability are the same for both HWs and

CWs and hazard is the only differing variable.

Figure 6-a (Figure 6-b) show increasing trends in risk (due to change in vulnerability

455   only) in the main cities and nearby areas. Decreasing trends are found for most of the

remaining region.

Figure 6-c (Figure 6-d) show increasing trends in risk (due to change in exposure only)

in/near urban areas and decreasing trends in zones at high elevations and far from the

urban centers.

460   Figure 6-d show that the hazard is the main driver of risk for HWs, with statistically

significant increasing trends, more evident in and around highly populated areas.

Finally, Figure 6-e show no significant trends in CWs risk (due to change in hazards

only).
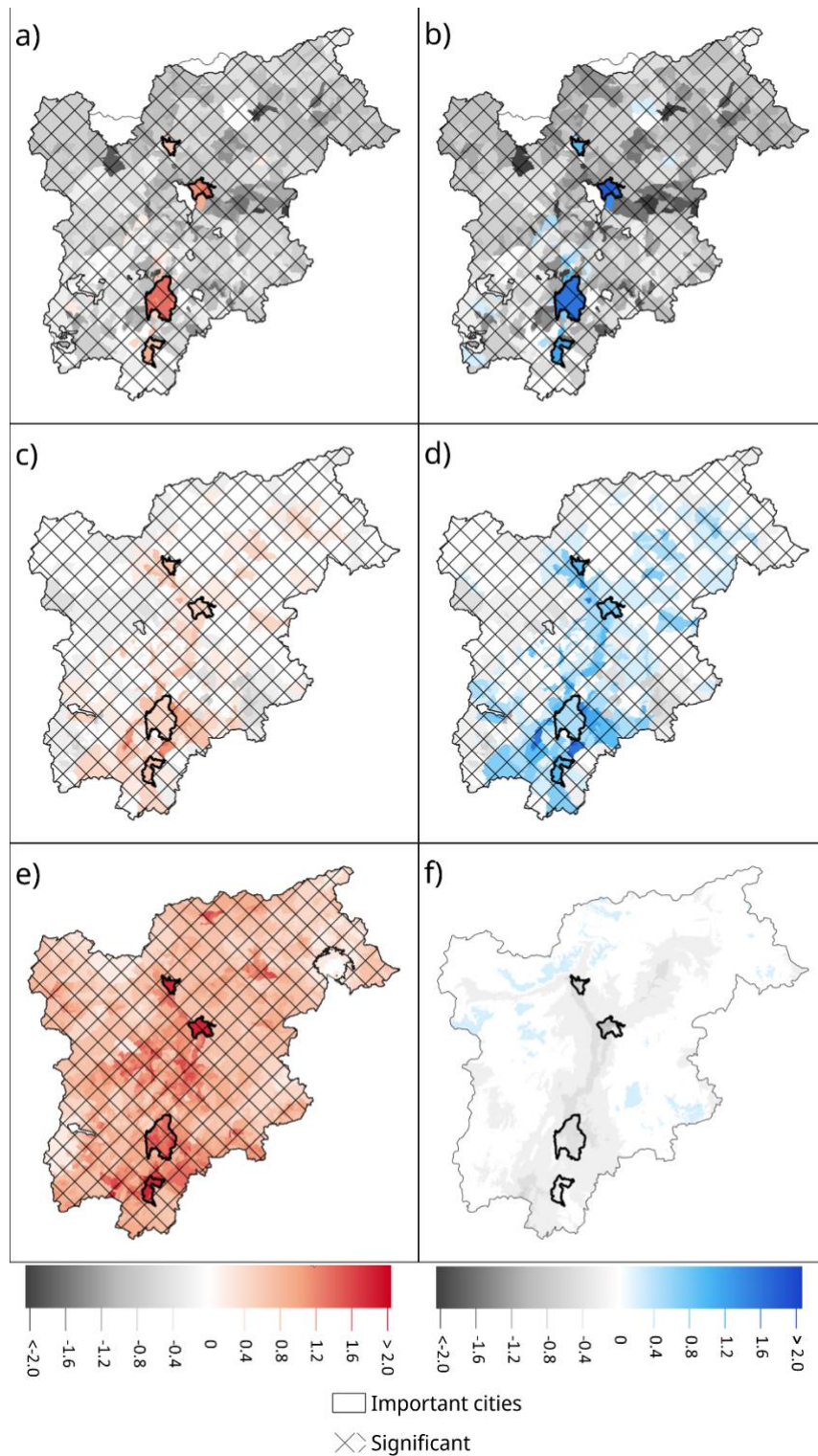
465   Figure 6: Trends of heat waves (and cold waves) risks due to changes in: a (b)

vulnerability only, c (d) exposure only, and e (f) hazard only. Trends found with the

robust linear method, colors indicating an increase in the risk and grey a decrease, significance is indicated with the hashing, the yearly change being the robust linear model coefficient.

5   Discussion

The years found with the greatest HWs for the region agree with those of Russo et al. (2015), who found very high HWs in 1983, 2003 and 2015 in their analysis of the ten greatest HWs in Europe since 1950. The fact that four of the six largest HWs occurred in the last decade suggests that climate change is already influencing the intensity and frequency of HWs in the Trentino Alto-Adige region. With regards to CWs, Jarzyna & Krzyżewska, (2021), have also found cold spells in the years 1985 and 2012 using different methodologies for other locations throughout Europe. Similarly, other studies have found 1985 to be a year of an exceptional CW in Europe (Spinoni et al., 2015; Twardosz and Kossowska-Cezak, 2016).

The significant increasing trend we found in HWs events are consistent with other studies in Europe over the last decades (e.g. Perkins-Kirkpatrick and Lewis, 2020; Piticar et al., 2018; Serrano-Notivoli et al., 2022; Spinoni et al., 2015; Zhang et al., 2020). The location of our highest increasing trends in HWs events are concordant to those of the higher increase in temperatures found at higher elevations by Acquaotta et al., (2015) in north-west Italy. Our results for HWs are also in line with the finding of Bacco et al., (2021) that analyzed trends in temperature extremes over northeastern regions of Italy (including Trentino Alto-Adige) based on homogenized data from dense station networks. They also found widespread warming, with significant positive trends

in maximum-related mean and daytime temperature extremes. The lack of trend in CWs

490   events is also in agreement with previous research that could not detect any trend in

extreme cold spells (Jarzyna and Krzyżewska, 2021; Piticar et al., 2018).

The trends in vulnerability and their absence of statical significance strongly depend on

the available data. In our case they are the output of specific national census carried out

every ten years and aggregated at the city spatial scale. From the other side, these data

495   represent a freely available option to quantify the vulnerability to natural hazards, which

is a crucial component for the risk quantification (e.g. Formetta and Feyen, 2019,

Frigerio & De Amicis, 2016).

The two driving factors behind the increase in vulnerability (elderly population and

isolation) have also been found as some of the main factors for vulnerabilities in other

500   regions of Europe (López-Bueno et al., 2021; Poumadère et al., 2005). The results of

our vulnerability analysis contrast with the findings of Frigerio & De Amicis (2016), who

report increasing vulnerabilities for municipalities of the Bolzano province and slightly

decreasing to steady vulnerabilities in the Trento province. This contrast, between our

finding and theirs, is related to the use of different indicators (employment, social-

505   economic status, family structures, race/ethnicity, and population growth) and a different

methodology for calculating the vulnerability where the normalization of indicators is

applied across all of Italy in their study, as opposed to only over the Trentino Alto-Adige

region in this study, the latter characterizing better local vulnerability. The selection of

different indicators and methodology might yield different results.

510   Our findings related to the increase in HWs risks are consistent with Smid et al., (2019),

which showed an increase of risk in both current and the future period for European

capitals; the same study highlights a future decrease in CWs risk for these same cities.

We found that CWs risk is still increasing for the main cities of our study. This is also the

case for other cities in mountainous regions, such as highlighted by López-Bueno et al.

515   (2021) for the city of Madrid, where the urban area was found to be the more at CWs

risk compared to the rural area.

The analysis of the trends of risk while changing only one of its three variables and

keeping constant the remaining two shows that hazard and vulnerability are the main

driving factor of the HWs risk. The changes in HWs risk due to hazard also highlights

520   the presence of urban heat island in the most populated cities of the region (in Figure 6-

e these are the zones of the highest increasing trends in risk). This has also been found

in other in urban areas (e.g. Morabito et al., 2021). The changes in CWs risk is mainly

explained by the demographic and vulnerability changes, which are increasing

in/around urban areas and decreasing elsewhere.

525   The changes found in HWs and CWs risk due to changes in exposure or vulnerability

only is partially explained by rural-urban migration and an aging population, which is

presented in other studies such as (Reynaud and Miccoli, 2018).

6   Summary and conclusions

Our study is one of the first to calculate risks of HWs and CWs and their trends at the

530   community and city level for a region over 39 years. This is done by first quantifying the

historical hazard of extreme temperature events using the HWMId and CWMId

indicators, at high spatial resolution (250 m) in the Trentino Alto-Adige region for the

period 1980-2018. The hazard probability of occurrences are then quantified by fitting a

Tweedie distribution to the HWMId and CWMId values, explicitly accounting for zero

535   values in their time series. Two types of population exposure are found using the

different hazard levels (5 years and 10 years return level). Vulnerability is calculated

using 8 different socioeconomic indicators. Combining all these findings, the spatio-

temporal HWs / CWs risk over the time-period and at the city level is calculated.

Over the past 4 decades, HWs, i.e. HWMId>0, (and extreme HWs, i.e. HWMId>HW5Y)

540   showed increasing trends in most of the region, with 98% (70%) being statistically

significant. This results in an increasing exposure of people to extreme heat spells. For

CW, we did not find a trend in hazard frequency and intensity and exposure to extreme

cold remain constant. With regards to risk, in the region in general a steady increase

(~12%) in HWs risk and a decrease (~7%) in CWs risk are found. However, in the larger

545   cities of the region, a much stronger rise in HWs risk (~45%) and CWs risk (~17%)

occur. This is linked with demographic changes and the social status of city inhabitants,

with more people and an ageing population living in cities and an increase in the

number of people living alone.

The findings of this work shows that municipalities and cities in the Trentino Alto-Adige

550   region have been seen increasing trends in HWs risk over the timeframe 1980-2018,

while potentially experiencing the same levels of CWs risk. Our detailed analysis shows

where to prioritize risk mitigation measures to reduce the hazard and vulnerability.

Measures to mitigate heat in cities include, for example, greening of cities (Alsaad et al.,

2022; Taleghani et al., 2019), while vulnerability could be decreased by improving the

555   social and living conditions of citizens, especially of the elderly who are more vulnerable

(Orlando et al., 2021; Poumadère et al., 2005; Vu et al., 2019), particularly in the cities

of this region where they are becoming more numerous. If detailed data are available

for temperature, exposure and vulnerability indicators, the methodology presented here

could be applied to other regions in- and outside Italy to help steer local climate

560   adaptation investments at the city level.

Code availability

The code used for calculating HWMId and CWMId is free and open source, it is the

extRemes package of R which is findable here: https://cran.r-

565   project.org/package=extRemes.

Data availability

All data used in this study is available freely and openly online. The temperature

data(Crespi et al., 2021) is available at the following location:

https://doi.pangaea.de/10.1594/PANGAEA.924502. The population data from the GHSL

570   is available at this location: https://data.jrc.ec.europa.eu/collection/ghsl. The indicator

data used to calculate the vulnerable is available from ISTAT: https://www.istat.it/en/.

575

References

Acquaotta, F., Fratianni, S., and Garzena, D.: Temperature changes in the North-Western Italian Alps from 1961 to 2010, Theor. Appl. Climatol., 122, 619–634, https://doi.org/10.1007/s00704-014-1316-7, 2015.

580   Alsaad, H., Hartmann, M., Hilbel, R., and Voelker, C.: The potential of facade greening in mitigating the effects of heatwaves in Central European cities, Build. Environ., 216, 109021, https://doi.org/10.1016/j.buildenv.2022.109021, 2022.

Bacco, M. D. and Scorzini, A. R.: Recent changes in temperature extremes across the north-eastern region of Italy and their relationship with large-scale circulation, Clim.

585   Res., 81, 167–185, https://doi.org/10.3354/cr01614, 2020.

Bonat, W. H. and Kokonendji, C. C.: Flexible Tweedie regression models for continuous data, J. Stat. Comput. Simul., 87, 2138–2152, https://doi.org/10.1080/00949655.2017.1318876, 2017.

Buscail, C., Upegui, E., and Viel, J.-F.: Mapping heatwave health risk at the community

590   level for public health action, Int. J. Health Geogr., 11, 38, https://doi.org/10.1186/1476-072X-11-38, 2012.

Buzási, A.: Comparative assessment of heatwave vulnerability factors for the districts of Budapest, Hungary, Urban Clim., 42, 101127, https://doi.org/10.1016/j.uclim.2022.101127, 2022.

595   Ceccherini, G., Russo, S., Ameztoy, I., Marchese, A. F., and Carmona-Moreno, C.: Heat waves in Africa 1981–2015, observations and reanalysis, Nat. Hazards Earth Syst. Sci., 17, 115–125, https://doi.org/10.5194/nhess-17-115-2017, 2017.

Chambers, J.: Global and cross-country analysis of exposure of vulnerable populations to heatwaves from 1980 to 2018, Clim. Change, 163, 539–558,

600   https://doi.org/10.1007/s10584-020-02884-2, 2020.

Cheng, W., Li, D., Liu, Z., and Brown, R. D.: Approaches for identifying heat-vulnerable populations and locations: A systematic review, Sci. Total Environ., 799, 149417, https://doi.org/10.1016/j.scitotenv.2021.149417, 2021.

Conti, S., Meli, P., Minelli, G., Solimini, R., Toccaceli, V., Vichi, M., Beltrano, C., and

605   Perini, L.: Epidemiologic study of mortality during the Summer 2003 heat wave in Italy, Environ. Res., 98, 390–399, https://doi.org/10.1016/j.envres.2004.10.009, 2005.

Crespi, A., Matiu, M., Bertoldi, G., Petitta, M., and Zebisch, M.: A high-resolution gridded dataset of daily temperature and precipitation records (1980–2018) for Trentino – South Tyrol (north-eastern Italian Alps), Earth Syst. Sci. Data

610   Discuss., 1–27, https://doi.org/10.5194/essd-2020-346, 2021.

de'Donato, F. K., Leone, M., Noce, D., Davoli, M., and Michelozzi, P.: The Impact of the February 2012 Cold Spell on Health in Italy Using Surveillance Data, PLOS ONE, 8, e61720, https://doi.org/10.1371/journal.pone.0061720, 2013.

Dong, J., Peng, J., He, X., Corcoran, J., Qiu, S., and Wang, X.: Heatwave-induced

615   human health risk assessment in megacities based on heat stress-social vulnerability-

human exposure framework, Landsc. Urban Plan., 203, 103907, https://doi.org/10.1016/j.landurbplan.2020.103907, 2020.

Dosio, A., Mentaschi, L., Fischer, E. M., and Wyser, K.: Extreme heat waves under 1.5\hspace0.167em°C and 2\hspace0.167em°C global warming, Environ. Res. Lett., 13, 054006, https://doi.org/10.1088/1748-9326/aab827, 2018.

Dunn, P. K.: Occurrence and quantity of precipitation can be modelled simultaneously, Int. J. Climatol., 24, 1231–1239, https://doi.org/10.1002/joc.1063, 2004.

Dunn, P. K.: tweedie: Evaluation of Tweedie Exponential Family Models, 2021.

Ellena, M., Ballester, J., Mercogliano, P., Ferracin, E., Barbato, G., Costa, G., and Ingole, V.: Social inequalities in heat-attributable mortality in the city of Turin, northwest of Italy: a time series analysis from 1982 to 2018, Environ. Health, 19, 116, https://doi.org/10.1186/s12940-020-00667-x, 2020.

El-Zein, A. and Tonmoy, F. N.: Assessment of vulnerability to climate change using a multi-criteria outranking approach with application to heat stress in Sydney, Ecol. Indic., 48, 207–217, https://doi.org/10.1016/j.ecolind.2014.08.012, 2015.

Estoque, R. C., Ooba, M., Seposo, X. T., Togawa, T., Hijioka, Y., Takahashi, K., and Nakamura, S.: Heat health risk assessment in Philippine cities using remotely sensed data and social-ecological indicators, Nat. Commun., 11, 1581, https://doi.org/10.1038/s41467-020-15218-8, 2020.

635   Formetta, G. and Feyen, L.: Empirical evidence of declining global vulnerability to

climate-related hazards, Glob. Environ. Change, 57, 101920,

https://doi.org/10.1016/j.gloenvcha.2019.05.004, 2019.

Fratianni, S. and Acquaotta, F.: The Climate of Italy, in: Landscapes and Landforms of

Italy, edited by: Soldati, M. and Marchetti, M., Springer International Publishing, Cham,

640   29–38, https://doi.org/10.1007/978-3-319-26194-2_4, 2017.

Frigerio, I. and De Amicis, M.: Mapping social vulnerability to natural hazards in Italy: A

suitable tool for risk mitigation strategies, Environ. Sci. Policy, 63, 187–196,

https://doi.org/10.1016/j.envsci.2016.06.001, 2016.

García-León, D., Casanueva, A., Standardi, G., Burgstall, A., Flouris, A. D., and Nybo,

645   L.: Current and projected regional economic impacts of heatwaves in Europe, Nat.

Commun., 12, 5807, https://doi.org/10.1038/s41467-021-26050-z, 2021.

Gasparrini, A., Guo, Y., Hashizume, M., Lavigne, E., Zanobetti, A., Schwartz, J., Tobias,

A., Tong, S., Rocklöv, J., Forsberg, B., Leone, M., Sario, M. D., Bell, M. L., Guo, Y.-L.

L., Wu, C., Kan, H., Yi, S.-M., Coelho, M. de S. Z. S., Saldiva, P. H. N., Honda, Y., Kim,

650   H., and Armstrong, B.: Mortality risk attributable to high and low ambient temperature: a

multicountry observational study, The Lancet, 386, 369–375,

https://doi.org/10.1016/S0140-6736(14)62114-0, 2015.

Goffard, P.-O., Jammalamadaka, S. R., and Meintanis, S.: Goodness-of-fit tests for

compound distributions with applications in insurance, 2019.

655   Habeeb, D., Vargo, J., and Stone, B.: Rising heat wave trends in large US cities, Nat. Hazards, 76, 1651–1665, https://doi.org/10.1007/s11069-014-1563-z, 2015.

Hasan, M. M. and Dunn, P. K.: Two Tweedie distributions that are near-optimal for modelling monthly rainfall in Australia, Int. J. Climatol., 31, 1389–1397, https://doi.org/10.1002/joc.2162, 2011.

660   Ho, H. C., Knudby, A., Chi, G., Aminipouri, M., and Lai, D. Y.-F.: Spatiotemporal analysis of regional socio-economic vulnerability change associated with heat risks in Canada, Appl. Geogr., 95, 61–70, https://doi.org/10.1016/j.apgeog.2018.04.015, 2018.

Huber, P. J.: Robust Statistics, in: International Encyclopedia of Statistical Science, edited by: Lovric, M., Springer, Berlin, Heidelberg, 1248–1251,

665   https://doi.org/10.1007/978-3-642-04898-2_594, 2011.

IPCC: Climate Change 2014 – Impacts, Adaptation and Vulnerability: Part A: Global and Sectoral Aspects: Working Group II Contribution to the IPCC Fifth Assessment Report: Volume 1: Global and Sectoral Aspects, Cambridge University Press, Cambridge, https://doi.org/10.1017/CBO9781107415379, 2014.

670   Istat.it - 15° Censimento della popolazione e delle abitazioni 2011: https://www.istat.it/it/censimenti-permanenti/censimenti-precedenti/popolazione-e-abitazioni/popolazione-2011, last access: 16 November 2021.

Jarzyna, K. and Krzyżewska, A.: Cold spell variability in Europe in relation to the degree of climate continentalism in 1981–2018 period, Weather, 76, 122–128,

675   https://doi.org/10.1002/wea.3937, 2021.

Johnson, W. D., Burton, J. H., Beyl, R. A., and Romer, J. E.: A Simple Chi-Square Statistic for Testing Homogeneity of Zero-Inflated Distributions, Open J. Stat., 5, 483, https://doi.org/10.4236/ojs.2015.56050, 2015.

Jorgensen, B.: Exponential Dispersion Models, J. R. Stat. Soc. Ser. B Methodol., 49, 127–162, 1987.

Karanja, J. and Kiage, L.: Perspectives on spatial representation of urban heat vulnerability, Sci. Total Environ., 774, 145634, https://doi.org/10.1016/j.scitotenv.2021.145634, 2021.

Kim, D.-W., Deo, R. C., Lee, J.-S., and Yeom, J.-M.: Mapping heatwave vulnerability in Korea, Nat. Hazards, 89, 35–55, https://doi.org/10.1007/s11069-017-2951-y, 2017.

King, A. D., Donat, M. G., Lewis, S. C., Henley, B. J., Mitchell, D. M., Stott, P. A., Fischer, E. M., and Karoly, D. J.: Reduced heat exposure by limiting global warming to 1.5 °C, Nat. Clim. Change, 8, 549–551, https://doi.org/10.1038/s41558-018-0191-0, 2018.

Kishore, P., Basha, G., Venkat Ratnam, M., AghaKouchak, A., Sun, Q., Velicogna, I., and Ouarda, T. B. J. M.: Anthropogenic influence on the changing risk of heat waves over India, Sci. Rep., 12, 3337, https://doi.org/10.1038/s41598-022-07373-3, 2022.

Kron, W., Löw, P., and Kundzewicz, Z. W.: Changes in risk of extreme weather events in Europe, Environ. Sci. Policy, 100, 74–83, https://doi.org/10.1016/j.envsci.2019.06.007, 2019.

Liu, X., Yue, W., Yang, X., Hu, K., Zhang, W., and Huang, M.: Mapping Urban Heat Vulnerability of Extreme Heat in Hangzhou via Comparing Two Approaches, Complexity, 2020, e9717658, https://doi.org/10.1155/2020/9717658, 2020.

700 López-Bueno, J. A., Navas-Martín, M. Á., Díaz, J., Mirón, I. J., Luna, M. Y., Sánchez-Martínez, G., Culqui, D., and Linares, C.: The effect of cold waves on mortality in urban and rural areas of Madrid, Environ. Sci. Eur., 33, 72, https://doi.org/10.1186/s12302-021-00512-z, 2021.

Michelozzi, P., de 'Donato, F., Bisanti, L., Russo, A., Cadum, E., DeMaria, M., D'Ovidio, M., Costa, G., and Perucci, C. A.: Heat Waves in Italy: Cause Specific Mortality and the
705 Role of Educational Level and Socio-Economic Conditions, in: Extreme Weather Events and Public Health Responses, edited by: Kirch, W., Bertollini, R., and Menne, B., Springer, Berlin, Heidelberg, 121–127, https://doi.org/10.1007/3-540-28862-7_12, 2005.

Michelozzi, P., De' Donato, F., Scortichini, M., De Sario, M., Asta, F., Agabiti, N., Guerra, R., de Martino, A., and Davoli, M.: [On the increase in mortality in Italy in 2015:
710 analysis of seasonal mortality in the 32 municipalities included in the Surveillance system of daily mortality], Epidemiol. Prev., 40, 22–28, https://doi.org/10.19191/EP16.1.P022.010, 2016.

Morabito, M., Crisci, A., Gioli, B., Gualtieri, G., Toscano, P., Stefano, V. D., Orlandini, S., and Gensini, G. F.: Urban-Hazard Risk Analysis: Mapping of Heat-Related Risks in
715 the Elderly in Major Italian Cities, PLOS ONE, 10, e0127277, https://doi.org/10.1371/journal.pone.0127277, 2015.

Morabito, M., Crisci, A., Guerri, G., Messeri, A., Congedo, L., and Munafò, M.: Surface urban heat islands in Italian metropolitan cities: Tree cover and impervious surface influences, Sci. Total Environ., 751, 142334,

720   https://doi.org/10.1016/j.scitotenv.2020.142334, 2021.

Neumayer, E. and Barthel, F.: Normalizing economic loss from natural disasters: A global analysis, Glob. Environ. Change, 21, 13–24, https://doi.org/10.1016/j.gloenvcha.2010.10.004, 2011.

Oldenborgh, G. J. van, Mitchell-Larson, E., Vecchi, G. A., Vries, H. de, Vautard, R., and

725   Otto, F.: Cold waves are getting milder in the northern midlatitudes, Environ. Res. Lett., 14, 114004, https://doi.org/10.1088/1748-9326/ab4867, 2019.

Orlando, S., Mosconi, C., De Santo, C., Emberti Gialloreti, L., Inzerilli, M. C., Madaro, O., Mancinelli, S., Ciccacci, F., Marazzi, M. C., Palombi, L., and Liotta, G.: The Effectiveness of Intervening on Social Isolation to Reduce Mortality during Heat Waves

730   in Aged Population: A Retrospective Ecological Study, Int. J. Environ. Res. Public. Health, 18, 11587, https://doi.org/10.3390/ijerph182111587, 2021.

Papathoma-Köhle, M., Ulbrich, T., Keiler, M., Pedoth, L., Totschnig, R., Glade, T., Schneiderbauer, S., and Eidswig, U.: Chapter 8 - Vulnerability to Heat Waves, Floods, and Landslides in Mountainous Terrain: Test Cases in South Tyrol, in: Assessment of

735   Vulnerability to Natural Hazards, edited by: Birkmann, J., Kienberger, S., and Alexander, D. E., Elsevier, 179–201, https://doi.org/10.1016/B978-0-12-410528-7.00008-4, 2014.

Peng, J., Liu, Y., Li, T., and Wu, J.: Regional ecosystem health response to rural land use change: A case study in Lijiang City, China, Ecol. Indic., 72, 399–410,

740   https://doi.org/10.1016/j.ecolind.2016.08.024, 2017.

Perkins-Kirkpatrick, S. E. and Gibson, P. B.: Changes in regional heatwave characteristics as a function of increasing global temperature, Sci. Rep., 7, 12256, https://doi.org/10.1038/s41598-017-12520-2, 2017.

Perkins-Kirkpatrick, S. E. and Lewis, S. C.: Increasing trends in regional heatwaves,

745   Nat. Commun., 11, 3357, https://doi.org/10.1038/s41467-020-16970-7, 2020.

Piticar, A., Croitoru, A.-E., Ciupertea, F.-A., and Harpa, G.-V.: Recent changes in heat waves and cold waves detected based on excess heat factor and excess cold factor in Romania, Int. J. Climatol., 38, 1777–1793, https://doi.org/10.1002/joc.5295, 2018.

Poumadère, M., Mays, C., Le Mer, S., and Blong, R.: The 2003 Heat Wave in France:

750   Dangerous Climate Change Here and Now, Risk Anal., 25, 1483–1494, https://doi.org/10.1111/j.1539-6924.2005.00694.x, 2005.

Quader, M. A., Khan, A. U., and Kervyn, M.: Assessing Risks from Cyclones for Human Lives and Livelihoods in the Coastal Region of Bangladesh, Int. J. Environ. Res. Public. Health, 14, E831, https://doi.org/10.3390/ijerph14080831, 2017.

755   Rahma, A. and Kokonendji, C. C.: Discriminating between and within (semi)continuous classes of both Tweedie and geometric Tweedie models, J. Stat. Comput. Simul., 2021.

Reid, C. E., O'Neill Marie S., Gronlund Carina J., Brines Shannon J., Brown Daniel G., Diez-Roux Ana V., and Schwartz Joel: Mapping Community Determinants of Heat Vulnerability, Environ. Health Perspect., 117, 1730–1736,

760   https://doi.org/10.1289/ehp.0900683, 2009.

Reynaud, C. and Miccoli, S.: Depopulation and the Aging Population: The Relationship in Italian Municipalities, Sustainability, 10, 1004, https://doi.org/10.3390/su10041004, 2018.

Russo, S., Sillmann, J., and Fischer, E. M.: Top ten European heatwaves since 1950

765   and their occurrence in the coming decades, Environ. Res. Lett., 10, 124003, https://doi.org/10.1088/1748-9326/10/12/124003, 2015.

Russo, S., Marchese, A. F., Sillmann, J., and Immé, G.: When will unusual heat waves become normal in a warming Africa?, Environ. Res. Lett., 11, 054016, https://doi.org/10.1088/1748-9326/11/5/054016, 2016.

770   Russo, S., Sillmann, J., Sippel, S., Barcikowska, M. J., Ghisetti, C., Smid, M., and O'Neill, B.: Half a degree and rapid socioeconomic development matter for heatwave risk, Nat. Commun., 10, 136, https://doi.org/10.1038/s41467-018-08070-4, 2019.

Schiavina, M., Freire, S., and MacManus, K.: GHS-POP R2019A - GHS population grid multitemporal (1975-1990-2000-2015), https://doi.org/10.2905/0C6B9751-A71F-4062-

775   830B-43C9F432370F, 2019.

Serrano-Notivoli, R., Lemus-Canovas, M., Barrao, S., Sarricolea, P., Meseguer-Ruiz, O., and Tejedor, E.: Heat and cold waves in mainland Spain: Origins, characteristics,

and trends, Weather Clim. Extrem., 37, 100471,

https://doi.org/10.1016/j.wace.2022.100471, 2022.

780   Shono, H.: Application of the Tweedie distribution to zero-catch data in CPUE analysis,

Fish. Res., 93, 154–162, https://doi.org/10.1016/j.fishres.2008.03.006, 2008.

Smid, M., Russo, S., Costa, A. C., Granell, C., and Pebesma, E.: Ranking European

capitals by exposure to heat waves and cold waves, Urban Clim., 27, 388–402,

https://doi.org/10.1016/j.uclim.2018.12.010, 2019.

785   Spinoni, J., Lakatos, M., Szentimrey, T., Bihari, Z., Szalai, S., Vogt, J., and Antofie, T.:

Heat and cold waves trends in the Carpathian Region from 1961 to 2010, Int. J.

Climatol., 35, 4197–4209, https://doi.org/10.1002/joc.4279, 2015.

Taleghani, M., Marshall, A., Fitton, R., and Swan, W.: Renaturing a microclimate: The

impact of greening a neighbourhood on indoor thermal comfort during a heatwave in

790   Manchester, UK, Sol. Energy, 182, 245–255,

https://doi.org/10.1016/j.solener.2019.02.062, 2019.

Temple, S. D.: The Tweedie Index Parameter and Its Estimator An Introduction with

Applications to Actuarial Ratemaking, 2018.

Tijdeman, E., Stahl, K., and Tallaksen, L. M.: Drought Characteristics Derived Based on

795   the Standardized Streamflow Index: A Large Sample Comparison for Parametric and

Nonparametric Methods, Water Resour. Res., 56,

https://doi.org/10.1029/2019WR026315, 2020.

Tuholske, C., Caylor, K., Funk, C., Verdin, A., Sweeney, S., Grace, K., Peterson, P., and Evans, T.: Global urban population exposure to extreme heat, Proc. Natl. Acad.

800   Sci., 118, e2024792118, https://doi.org/10.1073/pnas.2024792118, 2021.

Twardosz, R. and Kossowska-Cezak, U.: Exceptionally cold and mild winters in Europe (1951–2010), Theor. Appl. Climatol., 125, 399–411, https://doi.org/10.1007/s00704-015-1524-9, 2016.

Tweedie, M. C. K.: An index which distinguishes between some important exponential

805   families, in: Statistics: applications and new directions (Calcutta, 1981), Indian Statist. Inst., Calcutta, 579–604, 1984.

Disaster risk: https://www.undrr.org/terminology/disaster-risk, last access: 21 November 2021.

Vu, A., Rutherford, S., and Phung, D.: Heat Health Prevention Measures and

810   Adaptation in Older Populations—A Systematic Review, Int. J. Environ. Res. Public. Health, 16, 4370, https://doi.org/10.3390/ijerph16224370, 2019.

Watts, N., Amann, M., Arnell, N., Ayeb-Karlsson, S., Belesova, K., Berry, H., Bouley, T., Boykoff, M., Byass, P., Cai, W., Campbell-Lendrum, D., Chambers, J., Daly, M., Dasandi, N., Davies, M., Depoux, A., Dominguez-Salas, P., Drummond, P., Ebi, K. L.,

815   Ekins, P., Montoya, L. F., Fischer, H., Georgeson, L., Grace, D., Graham, H., Hamilton, I., Hartinger, S., Hess, J., Kelman, I., Kiesewetter, G., Kjellstrom, T., Kniveton, D., Lemke, B., Liang, L., Lott, M., Lowe, R., Sewe, M. O., Martinez-Urtaza, J., Maslin, M., McAllister, L., Mikhaylov, S. J., Milner, J., Moradi-Lakeh, M., Morrissey, K., Murray, K.,

Nilsson, M., Neville, T., Oreszczyn, T., Owfi, F., Pearman, O., Pencheon, D., Pye, S.,

820   Rabbaniha, M., Robinson, E., Rocklöv, J., Saxer, O., Schütte, S., Semenza, J. C.,

Shumake-Guillemot, J., Steinbach, R., Tabatabaei, M., Tomei, J., Trinanes, J., Wheeler,

N., Wilkinson, P., Gong, P., Montgomery, H., and Costello, A.: The 2018 report of the

Lancet Countdown on health and climate change: shaping the health of nations for

centuries to come, The Lancet, 392, 2479–2514, https://doi.org/10.1016/S0140-

825   6736(18)32594-7, 2018.

Zhang, R., Sun, C., Zhu, J., Zhang, R., and Li, W.: Increased European heat waves in

recent decades in response to shrinking Arctic sea ice and Eurasian snow cover, Npj

Clim. Atmospheric Sci., 3, 1–9, https://doi.org/10.1038/s41612-020-0110-8, 2020.